Molecular and functional regionalization of bicarbonate secretion cascade in the intestine of the European sea bass (*Dicentrarchus labrax*)

*Alexandra Alves, Sílvia F Gregório, Renata C Egger & Juan Fuentes**

KEY WORDS: HCO_3^- secretion, intestine, ion transport, marine fish, regionalization, sea bass

Short title: Regionalization of sea bass intestine

* Author for correspondence:

Juan Fuentes (jfuentes@ualg.pt)

Centre of Marine Sciences (CCMar)

Universidade do Algarve

Campus de Gambelas,

8005-139 Faro, Portugal

Tel: 00351289800900 ext: 7203

ABSTRACT

In marine fish the intestinal HCO_3^- secretion is the key mechanism to enable luminal aggregate formation and water absorption. Using the sea bass (*Dicentrarchus labrax)*, the present study aimed at establishing functional and molecular organization of different sections of the intestine in relation to bicarbonate secretion and Cl^- movements. The proximal intestinal regions presented similar HCO_3^- secretion rates, whilst differences were detected in the molecular expression of the transporters involved and on regional HCO_3^- concentrations. The anterior region presented significantly higher Na^+/K^+-ATPase activity, Cl^- transepithelial transport and basolateral slc4a4, apical slc26a6 and slc26a3 expression levels. In the mid intestine, the total HCO_3^- content was significantly increased in the fluid as in the carbonate aggregates. In the rectum no HCO_3^- secretion was observed and was characterized by the diminished HCO_3^- total content, residual molecular expression of slc4a4, slc26a6 and slc26a3, higher H^+-ATPase activity and expression, suggesting a different mechanism in bicarbonate handling. The possible regulation of HCO_3^- secretion by extracellular HCO_3^- and increased intracellular cAMP levels were investigated. The transcellular / intracellular dependence of apical HCO_3^- secretion differed between the proximal regions of the intestine. In addition, cAMP had no effect on HCO_3^- secretion, although Cl^- secretion was enhanced by cftr. HCO_3^- secretion rise due to the HCO_3^- basolateral increment showed that at resting levels slc4a4 was not a limiting step for apical secretion. In conclusion, intestinal HCO_3^- secretion has functional region-dependent organization that was not reflected by the anterior-posterior regionalization on HCO_3^- secretion and water absorption gene expression profiling.

INTRODUCTION

Marine fish suffer passive dehydration mainly through the gills by the action of the hyperosmotic surrounding environment (Evans, 2008; Marshall and Grosell, 2006; McCormick et al., 2013; Smith, 1931). To withstand this situation, fish drink high amounts of seawater (SW), absorb water and eliminate excess salts (Fuentes and Eddy, 1997). Since net water absorption in the intestine is precluded by the negative osmotic gradient in plasma in relation to SW, a complex processing of the ingested fluid is required to favor water absorption in the intestine. The desalting process of ingested SW starts in the esophagus by passive transport (Parmelee and Renfro, 1983) and continues through the intestine, where monovalent ions (mainly Na^+ and Cl^-) are removed from the lumen in a process driven by active transport (Smith, 1931), and are excreted through the gills (Evans, 2005).

Intestinal water absorption is driven by the inward NaCl movement through the apical $Na^+/K^+/2Cl^-$ cotransporter (NKCC2 / solute carrier family 12 member 1 - slc12a1) (Musch et al., 1982) by the action of the basolateral Na^+/K^+-ATPase. The ATPase establishes an electrochemical gradient that promotes Na^+, K^+ and Cl^- uptake by the apical membrane transporters NKCC2, Na^+/Cl^- cotransporter (NCC or slc12a3) and Cl^-/HCO_3^- exchangers (reviewed in Grosell and Genz, 2006). The continuous ingestion of SW leads to increased Cl^- concentration in the intestinal luminal fluid (Wilson et al., 2002). The Cl^- gradient formed, promotes the transepithelial Cl^- transport by apical anion exchangers such as slc26a6 and slc26a3 that belong to the slc26 family, which promotes simultaneous HCO_3^- secretion (Kurita et al., 2008). Moreover, intestinal HCO_3^- secretion increases alkalinity in the intestinal lumen, that in combination with the high concentrations of the divalent cations (Ca^{2+} and Mg^{2+}) generates carbonate precipitates (Walsh et al., 1991). An apical vacuolar-type H^+-ATPase (H^+-ATPase or V-ATPase) secretes acid to the intestinal lumen promoting Cl^-/HCO_3^- exchange by titration of apical HCO_3^- that generates an additional water molecule that is readily available for absorption (Guffey et al., 2011). The process that generates carbonate precipitates allows ion-driven water uptake across the intestinal epithelium due to the osmolality reduction of the processed fluid (Wilson et al., 2002).

HCO_3^- secretion pathways in marine teleosts are only partially described, although there is evidence of the existence of different pathways. Transepithelial movement of basolateral HCO_3^- is described in several species, as being mediated by Na^+/HCO_3^- cotransporter (slc4a4, or electrogenic sodium bicarbonate cotransporter 1 - NBCe1) present in the basolateral membrane. This ionic movement promotes HCO_3^- intracellular accumulation, which in turn will facilitate Cl^-/HCO_3^- exchange by the apical slc26 exchangers, representing the transcellular pathway (Ando and Subramanyam, 1990; Carvalho et al., 2012; Dixon and Loretz, 1986; Faggio et al., 2011; Fuentes et al., 2010; Grosell and Genz, 2006; Kurita et al., 2008; Taylor et al., 2010; Wilson and Grosell, 2003). However, apical HCO_3^- secretion is still observed in the absence of basolateral HCO_3^-, indicating that there is an intracellular contribution by CO_2 hydration in the enterocyte catalyzed by carbonic anhydrases, to fuel the apical Cl^-/HCO_3^- exchangers (Fuentes et al., 2010; Grosell et al., 2009a; Whittamore, 2012).

Intestinal HCO_3^- secretion has been described in several marine fishes, although in most of them no intestinal regionalization of this process is described, such is the case in Gulf toadfish, European flounder, Pacific sandhab and lemon sole (Grosell, 2006; Grosell et al., 2001; Wilson et al., 2002). Interestingly, in the case of the Gulf toadfish there are no significant differences between regional secretion rates, while the anion exchanger slc26a6 expression levels are region dependent and comparatively to the posterior intestine and the rectum, the slc26a6 relative expression levels are 2000 and 200-fold higher in the anterior and mid intestine, respectively (Grosell et al., 2009b). Moreover, the Na^+/K^+-ATPase activity also differs between anterior and posterior intestine in this species (Guffey et al., 2011). Meanwhile, in sea bream there is a functional intestinal anterior-posterior specialization (Gregorio et al., 2013). Regional differences in HCO_3^- secretion rates are accompanied by different transporter expression levels of slc26a3, slc4a4, atp6v1b (H^+-ATPase subunit β), Cystic fibrosis transmembrane conductance regulator (cftr) and basolateral $Na^+/K^+/2Cl^-$ cotransporter (NKCC1 or slc12a2), short-circuit currents (I_{SC}) and water absorption rates (Carvalho et al., 2012; Gregorio et al., 2013), or even the expression of aquaporins (Martos-Sitcha et al., 2015). In turn, SW tilapia has not only differences on regional HCO_3^- secretion, but also in regional

expression levels of slc26a3, slc26a6, slc4a4 and H^+-ATPase subunit C, demonstrating an intestinal regionalization between anterior, mid intestine and rectum (Ruiz-Jarabo et al., 2017).

In Teleosts, the functional structure of the digestive tract varies with diet, endocrine regulation, immune protection and osmoregulatory functions (Ando et al., 2003; Loretz, 1995). The European sea bass is an euryhaline marine teleost, with high economic importance in the Mediterranean area, being able to thrive in a wide range of salinity from freshwater to hypersalinity (Jensen et al., 1998). Therefore, the digestive tract regulates the anatomical as well as the functional response to salinity variations enabling the tolerance to drastic salinity changes (Giffard-Mena et al., 2006). In the sea bass intestine, a Na^+-dependent transport mechanism is responsible for HCO_3^- uptake by the basolateral membrane, indicated by the inhibition HCO_3^- secretion: with 4,4'-Diisothiocyano-2,2'-stilbenedisulfonic acid (DIDS), Na^+ substitution with choline in the basolateral saline, and the inhibition of Na^+/K^+-ATPase with ouabain (Faggio et al., 2011), suggesting that the slc4a4 is probably the transporter involved as suggested for the toadfish (Taylor et al., 2010). It was also demonstrated that the HCO_3^- secretion and net Cl^- transport are interconnected, since several inhibitory routes of HCO_3^- secretion contribute to significant modifications in the I_{SC}, in which the NKCC2 and Na^+/K^+-ATPase involvement were exposed in the mid intestine (Faggio et al., 2011). Following this work with sea bass, the present study aims at assessing i) HCO_3^- secretion in the discrete intestinal regions, ii) evaluate anterior-posterior intestinal ATPase activities, iii) establish the expression levels of molecular mechanisms of transporters involved in HCO_3^- secretion and water absorption, iv) determine the contribution of different pathways on apical HCO_3^- secretion (endogenous metabolic CO_2 and extracellular HCO_3^-), and v) the possible regulation of HCO_3^- secretion and Cl^- movement.

MATERIALS AND METHODS

Chemicals

All chemicals were of the highest grade and were obtained from Sigma-Aldrich (Madrid, Spain) unless stated otherwise. In experimental manipulations, forskolin (FK) and 3-isobutyl-1-

129 methylxanthine (IBMX) were used at 10 μM and 500 μM, respectively. Bafilomycin A1 was
130 acquired from Cayman Chemical (MI, USA), prepared as a concentrated stock at 30μM in H_2O and
131 used at 100 nM in the ATPase assay.
132
133 *Animals*
134 European sea bass (*Dicentrarchus labrax*) were obtained from the stock raised in Ramalhete
135 Experimental Marine Station (CCMar, University of Algarve, Faro, Portugal). At the experimental
136 time, the juveniles were allocated to 500 L SW tanks (36 ppt) with a maximum density of 6 kg m^{-3}.
137 The aerated recirculated circuits had biological filtration and 12h light / dark photoperiod. Fish were
138 fed daily at 1.5 - 2 % of body mass, and feeding was withheld for 36 h before sample collection to
139 ensure the absence of undigested food in the intestine. No mortality was observed during the
140 experiments.
141 All the experiments were conducted in compliance with the Guidelines of the European
142 Union (2010/63/UE) and the Portuguese legislation for the use of laboratory animals. All animal
143 protocols were performed under Group-C licenses from the Direcção-Geral de Veterinária,
144 Ministério da Agricultura, do Desenvolvimento Rural e das Pescas, Portugal.
145
146 *Plasma and intestinal fluid analysis*
147 Previous to all the experiments, and to allow *in vivo* conditions, 10 individuals were
148 anesthetized in SW containing 2-phenoxyethanol (1:5000), weighted and killed by decapitation, in
149 order to analyze blood and intestinal fluid composition. The blood was collected from the caudal
150 peduncle into heparinized syringes. Plasma was obtained by centrifugation (10,000 *g*, 3 min) and
151 stored at -20 ºC until analysis.
152 For HCO_3^- evaluation in intestinal fluid and aggregates, the intestinal content of unfed fish
153 was collected from the excised intestinal regions, emptied into pre-weighed vials and centrifuged
154 (10,000 g, 5 min) to separate fluid from precipitate. The fluid was transferred to pre-weighed vials
155 and the volume was measured to the nearest 0.1 μl (0.1 mg, assuming a density of 1). The

precipitates (observed in Fig.1) were weighed to the nearest 0.1 mg. Intestinal fluid and aggregates homogenate titratable alkalinity (HCO_3^- + CO_3^{2-}) was manually measured with the double titration method, as previously described (Gregorio et al., 2013). An aliquot of intestinal fluid was stored at -20 ºC for ion composition analysis.

Osmolality was measured with a Vapor Pressure Osmometer Model 5600 (Wescor, UT, USA). Plasma and intestinal fluid electrolytes (chloride, phosphorus, magnesium, and calcium) were measured by colorimetric assays, using commercial kits (Spinreact SA, Girona, Spain), with a Multi-Mode Microplate Reader BioTek Synergy™ 4 (BioTek® Instruments, Winooski, VT, USA). Sodium and potassium concentrations were determined with a flame photometer (BWB-XP PerformancePlus, BWB Technologies, UK).

Intestinal Bicarbonate Secretion

After anesthesia (see above) the sea bass abdominal region was exposed, the whole intestine was isolated with two mosquito forceps and divided into 3 sections (see Fig. 1): the anterior intestine, mid intestine and the rectum. Afterwards, the intestinal portions from all regions were mounted on a tissue holder (0.5 cm^2) and positioned in a Ussing chamber (P2400, Physiological Instruments, San Diego, USA) containing 2 ml of physiological saline. Saline composition was defined by plasma and intestinal fluid analysis as shown in Table 1 to simulate *in vivo* like conditions, the composition is shown in Table 2. The basolateral (plasma) side contained pre-gassed basolateral saline with pH 7.800 that was continuously mixed by bubbling through 0.3 % CO_2 + 99.7 % O_2. The apical side was continuously gassed with 100 % O_2, and the pH was maintained at 7.800 by pH-Stat. In the experiments in which $NaHCO_3$ was omitted from the basolateral saline, Na-HEPES was used as a replacement and mixed by bubbling with 100 % O_2. The temperature of the chambers was maintained constant at 22 °C in all the experiments.

All bioelectrical variables were monitored by means of Ag/AgCl electrodes (with tip asymmetry <1 mV) connected to either side of the Ussing chamber with 3-mm-bore agar bridges (KCl, 1 M in 3 % agar) and amplifiers with automatic fluid resistance compensation (VCC600,

183 Physiological Instruments, San Diego, USA). The transephetilial potential (TEP, mV) was
184 monitored under current clamp of epithelia (0 μA cm^{-2}), and transepithelial conductance (G_t, mS
185 cm^{-2}) was manually calculated using the voltage deflections induced by a biphasic 2 s pulse of 4 or
186 10 μA cm^{-2} every minute.
187 The characterization of HCO_3^- secretion was performed with the configuration of amplifier /
188 pH-STAT system on apical saline at a physiological pH of 7.800, as previously described by
189 Gregório et al. (2013), Grosell and Genz (2006) in sea bream and Gulf toadfish, respectively. The
190 preparations were left to attain a transepithelial steady-state voltage (generally around 1 hour), and
191 at least 30 min of stable control periods of HCO_3^- secretion. At which point, in the anterior and mid
192 intestine, the basolateral saline was replaced with different concentrations of $NaHCO_3$ (0, 10, 20
193 mM). The preparations were monitored for an experimental period of at least 60 min. The time and
194 the volume of acid titrant (HCl, 2.5 mM) were manually recorded, as well as the tissue bioelectric
195 properties. Total HCO_3^- secreted was calculated from the titrant volume, the titrant concentration
196 and the surface area, and is presented as nmol h^{-1} cm^{-2}.
197
198 *Short Circuit Current (I_{SC}) measurement*
199 The regional intestinal sections were mounted in Ussing chambers as described above.
200 During these experiments the tissue was positioned between two half- chambers containing 2 mL of
201 basolateral physiological saline (Table 2), bilaterally gassed with 0.3 % CO_2 + 99.7 % O_2. Short-
202 circuit current (I_{SC}, μA cm^{-2}) was monitored by clamping the epithelia to 0 mV and and expressed
203 as negative for absorption of anions, considering the voltage referenced to the apical side of the
204 preparation. Transepithelial conductance (G_t, mS cm^{-2}) was manually calculated (Ohm's law) using
205 the current deflection induced by a 2 mV pulse of 3 s every minute. After the achievement of a
206 steady state, usually between 30 - 40 min after mounting, bioelectrical parameters for each
207 preparation were recorded by means of a Lab-Trax-4 acquisition system (World Precision
208 Instruments, Sarasota, FL, USA) using LabScribe3 (iWorx Systems Inc., Dover, NH, USA). Once

basal values were recorded, FK (10 μM) and IBMX (500 μM) were added to both basolateral and apical side, and bioelectric parameters monitored for at least 40 min.

ATPase activity

The intestinal mucosa was sampled from the three sections by fine-point scissors, the tissue was placed in 100 μl of ice-cold SEI buffer (150 mM sucrose, 10 mM EDTA, 50 mM imidazole, pH 7.3) and immediately frozen in liquid nitrogen. Intestinal ATPase activities were determined using a method adapted from McCormick (1993). Briefly, the tissues in SEI with Na-deoxycholate were homogenized and diluted to an optimal protein concentration of 1mg ml^{-1}. Protein content was determined by Bradford Protein Assay (Bio-Rad Laboratories, Hercules, CA, USA) using BSA as reference. Na^+/K^+-ATPase activity was calculated by the difference between total ATP hydrolysis in the absence and presence of the specific inhibitor, ouabain (0.5 mM). The activity attributable to H^+-ATPase was determined in parallel by the difference between ATP hydrolysis in the presence of ouabain and in combination with the specific inhibitor Bafilomycin A1(100 nM). The enzyme specific activity was expressed in μmol ADP mg $protein^{-1}$ h^{-1}.

qPCR

Intestinal samples of anterior intestine, mid intestine and rectum (Fig. 1) were collected from individual fish, stored during 24 h in RNAlater at 4 ºC, and then at -20 ºC until utilized for RNA extraction (performed within one week). Total RNA was extracted with the Total RNA Kit I (E.Z.N.A., Omega Bio-tek, Norcross, GA, USA) and DNase supplementary treatment (DNA-free Kit - RNase-Free DNase I Set, Omega Bio-tek, Norcross, GA, USA) following the manufacturer instructions. After assessing RNA quantity and quality (NanoPhotometer NP80, IMPLEN GmbH, Munich, Germany), reverse transcription of RNA into cDNA was carried out using the RevertAid First Strand cDNA Synthesis Kit (Fermentas, Thermo Scientific, Barrington, IL, USA) with 1000 ng of total RNA in a reaction volume of 20 μl. The cDNA sequences of the genes of interest slc26a3, slc26a6, slc4a4, slc12a1, slc12a2, slc12a3-001 (NCC subunit α), slc12a3-002 (NCC subunit β), cftr

236 and atp6v1b (V-type H^+-ATPase subunit β) were extracted from the EST collection database at the
237 National Center of Biotechnology (NCBI, http://blast.ncbi.nlm.nih.gov/) using TBLASTn queries of
238 known protein or deduced protein sequences from other fish species, or from the sea bass
239 transcriptome database and Sea Blast Server at CCMAR (http://sea.ccmar.ualg.pt in Louro et al.,
240 2016). Extracted sequences were compared by multisequence alignment using Clustal X to establish
241 their identity (Larkin et al., 2007). Primer pairs were designed using the software Primer3
242 (http://frodo.wi.mit.edu/) running under the EBioX (http://www.ebioinformatics.org/) interface for
243 Macintosh. Table 3 shows primer sequences, amplicon sizes and NCBI accession numbers of the
244 target sequences. Amplicon identities were confirmed by sequencing (CCMar). Real-time qPCR
245 amplifications were performed in duplicate in a final volume of 10 µl with 5 µl PerfeCTa® SYBR®
246 Green SuperMix, ROX (Quanta BioSciences, MA, USA), around 100 ng cDNA, and 0.3 µM of each
247 forward and reverse primers (Table 3). Amplifications were performed in 96-well plates using the
248 BIO RAD CFX connect Real-time system (Bio-Rad Laboratories, Hercules, CA, USA) with the
249 following protocol: denaturation and enzyme activation step at 95 ºC for 2 min, followed by 40 cycles
250 of 95 ºC for 15 s, and primer-pair specific annealing temperature (60 ºC) for 10 s. After the
251 amplification phase, a temperature-determining dissociation step was carried out increasing gradually
252 5 ºC each 15 s, between the range of 60 – 95 ºC to assure the existence of a single product. For
253 normalization of cDNA loading all samples were run in parallel using 18S ribosomal RNA (Carvalho
254 et al., 2015; Ferlazzo et al., 2012; Gregorio et al., 2014, 2013). To estimate efficiencies, a standard
255 curve was generated for each primer pair from 10-fold serial dilutions (from 100 to 0.001 pg) from a
256 cDNA pool that included all the intestinal samples. Standard curves represented the cycle threshold
257 value as a function of the logarithm of the number of copies generated, defined arbitrarily as one copy
258 for the most diluted standard. All calibration curves exhibited correlation coefficients $R^2 > 0.99$, and
259 the corresponding real-time PCR efficiencies range between 95.8 – 104.4 %.
260
261 *Statistics*

All results are shown as mean ± standard error of the mean (mean ± SEM). After assessing homogeneity of variance and normality, statistical analysis of the data was carried out by using one-way analysis of variance (ANOVA) using intestinal region / basolateral HCO_3^- concentrations / ion concentration / osmolality as a factor of variance, followed by the *Bonferroni post hoc* test. When pharmacological tools (FK + IBMX) were used, in I_{SC} and HCO_3^- secretion experiments, a one-way ANOVA using treatment as a factor of variance and a two-way ANOVA using time and treatment as a factor of variance followed by *post hoc Bonferroni* t-test were used respectively (Prism 5.0, GraphPad Software for McIntosh). The level of significance was set at $p < 0.01$ or 0.05.

RESULTS

Plasma, intestinal fluid and carbonate aggregate analysis

Sea bass juveniles did not present differences between plasma and intestinal fluid osmolality 336 vs 337 mOsm Kg^{-1} respectively (Table 1). Plasma had significantly higher Na^+ and Cl^- concentrations, and in the intestinal fluid, higher levels of Mg^{2+} and Ca^{2+}were observed with concentrations 130 and 8.5-fold higher, respectively in relation to plasma. Significant differences in Na^+, Cl^+ and Mg^{2+} concentrations were observed in the fluid of discrete intestinal regions, that were reflected on regional osmolality. The anterior intestine presented higher Na^+ and Cl^- concentrations and lower Mg^{2+} content (Fig. 2). Intestinal fluid and carbonate aggregates showed significantly higher HCO_3^- concentrations in the mid intestine (Fig. 3). In this region the fluid HCO_3^- concentration averaged 46.0 mEq l^{-1}, whereas the anterior intestine and rectum presented approximately 23.5 and 21.0 mEq l^{-1}, respectively. Total HCO_3^- content in the carbonate aggregates was significantly higher in the mid intestine (3985 nEq body $mass^{-1}$) when compared to the anterior region and rectum (199.4 and 354.9 nEq body $mass^{-1}$, respectively), as pictured by Fig. 1.

Regional HCO_3^- secretion

Sea bass intestinal HCO_3^- secretion ranged between 350 – 500 nmol h^{-1} cm^{-2} in the anterior and mid intestine, significantly higher from the rectum, which did not virtually secrete HCO_3^- (Fig.

4). HCO_3^- secretion measurement in the rectum was challenging due to difficulty to achieve titrable pH. All regions showed significantly different TEP, in which the mid intestine presented significant lower values (-16.5 mV) and rectum the highest (-2.4 mV). The posterior regions presented significant different G_t, the mid intestine G_t was 16.5 mS cm^{-2} and in the rectum was 10.0 mS cm^{-2}. During the course of experiments with smaller fish, higher HCO_3^- secretion rates were recorded. Therefore, an additional analysis with fish of different sizes showed an allometric relationship between fish mass and HCO_3^- secretion rates.

The possible regulation of HCO_3^- secretion was accessed by extracellular HCO_3^- (Fig. 6) and by a second messenger (Fig. 7). To this end, basolateral saline with different HCO_3^- concentrations were tested in *in vivo*-like conditions to investigate the HCO_3^- source dependence (Fig. 6). In saline devoid of HCO_3^- / CO_2 apical HCO_3^- secretion was approximately 180 and 220 nmol h^{-1} cm^{-2} in the anterior and mid intestine, respectively. In both intestinal regions, increasing basolateral HCO_3^- concentrations promoted HCO_3^- secretion to levels that can be fitted to linear regressions with $R^2 > 0.976$. The mid intestine was the region selected to investigate the possible regulation of the HCO_3^- secretion by FK + IBMX (Fig. 7), being the intestinal region with larger surface area. HCO_3^- secretion was unaltered by the rise of cAMP levels, and TEP became significantly less negative by 54 %, this effect was long lasting and without modification of epithelial selectivity, expressed as G_t.

Regional short-circuit current

In all intestinal regions were observed a negative I_{SC} that in our experimental conditions represent absorption of anions (Fig. 5). The regional I_{SC} values became less negative towards the posterior region. The anterior intestine presented significant lower values, -16.6 μA cm^2, and rectum the highest, -2.6 μA cm^2. G_t was significantly different in all discrete regions of the intestine, being higher in the mid intestine (20.5 mS cm^{-2}) and lower in the rectum (11.5 mS cm^{-2}).

The regional effect of increased levels of cAMP on I_{SC} was investigated with the bilateral addition of FK and IBMX (Fig. 7). All discrete regions of the intestine started with absorptive I_{SC}.

316 The bilateral application resulted in a significant increase of I_{SC}, the currents became less absorptive
317 and in the case of the rectum the I_{SC} became secretory. However, significant regional differences
318 were not observed in the amplitude of response in both I_{SC} and G_t.
319
320 *Intestinal ATPase activity*
321 Na^+/K^+-ATPase and H^+-ATPase activities revealed significant differences between the
322 discrete intestinal regions of sea bass (Fig. 8). Na^+/K^+-ATPase activity was significantly higher in
323 the anterior intestine (9.20 μmol ADP mg protein^{-1} h^{-1}). In turn, H^+-ATPase activity was 63 - 76 %,
324 significantly higher in the rectum (3.10 μmol ADP mg protein^{-1} h^{-1}) when compared to the other
325 regions.
326
327 *Molecular expression of transporters*
328 The molecular expression level of different transporters involved in HCO_3^- secretion were
329 analysed, basolateral slc4a4 and slc12a2, and apical slc26a6 and slc26a3, as well as slc12a1,
330 slc12a3-001, slc12a3-002, cftr and atp6v1b (Fig. 9). All genes had significant expression in the
331 intestinal regions tested. The basolateral Na^+/HCO_3^- cotransporter, slc4a4 presented significantly
332 higher expression levels in the anterior intestine. Likewise, significantly higher expression levels of
333 both anion exchangers of the slc26 family, slc26a6 and slc26a3 were observed in the anterior
334 intestine. Whereas atp6v1b, slc12a2, slc12a3-001 and slc12a3-002 expression levels were
335 significantly higher in the rectum. Apical cftr had significantly higher expression levels in the mid
336 intestine and lower in the rectum. The apical slc12a1 was the only gene in which the regional
337 differences on expression levels were absent.
338
339 **DISCUSSION**
340 In sea bass, Faggio et al. (2011) demonstrated the viability of mid intestine preparations to
341 characterize HCO_3^- secretion using the pH-Stat method with Ringer - isotonic salines. Establishing
342 HCO_3^- secreted sources: intracellular and transcellular contribution, and revealing that the

343 basolateral HCO_3^- uptake was energized by the Na^+/K^+-ATPase driving force (Na^+-dependent
344 transport), and the action of slc4a4 transport.

345 Here, we aimed at the characterization of HCO_3^- secretion in *in vivo* like conditions in sea
346 bass discrete intestinal regions. According with the regional fluid composition, HCO_3^- content in
347 fluid and carbonate aggregates, apical HCO_3^- secretion rates and the tissues bioelectrical properties
348 a functional anterior-posterior regionalization was established. The regional significant differences
349 in intestinal fluid ionic composition reflected the processing of SW ingested (Fig. 2). HCO_3^-
350 concentrations in the lumen (Fig. 3), being a putative reflection of apical secretion in each region,
351 were within the range observed in other teleost (33 – 110 mM) (Grosell et al., 2001; Taylor and
352 Grosell, 2006; Whittamore, 2012). Furthermore, the analysis of total HCO_3^- content of fluid and
353 carbonate aggregates implied that the mid intestine accounted for the majority of HCO_3^- that was
354 secreted in the intestine. However, there were no differences in HCO_3^- secretion rates between the
355 anterior and mid intestine (Fig. 4), revealing that the mid intestine could have a relative more
356 important functional role due to its larger surface area (53 – 58 % intestinal total length, Fig. 1). Sea
357 bass HCO_3^- secretion rates measured by pH-Stat were within the range observed in other marine
358 teleost between 300 - 700 nmol h^{-1} cm^{-2}, with a region-dependent variation that contrasts with other
359 species that lack intestinal regionalization such as Gulf toadfish, European flounder, Pacific
360 sanddab and lemon sole (Grosell, 2011; Grosell et al., 2001; Grosell and Genz, 2006; Grosell and
361 Taylor, 2007; Wilson et al., 2002). Similarities with sea bream were registered in terms of
362 regionalization, although the sea bream rectum presented HCO_3^- secretion rates circa 200 nmol h^{-1}
363 cm^{-2} (Carvalho et al., 2012), whilst the sea bass rectum secretes no HCO_3^-.

364 The molecular expression analysis of genes involved not only in HCO_3^- secretion (slc4a4,
365 slc26a3 and slc26a6), but also genes involved in the ionic movement and water absorption
366 (basolateral slc12a2 and apical slc12a3-001, slc12a3-002, cftr and atp6v1b) revealed an anterior-
367 posterior regionalization (Fig. 9). Interestingly, the regional specialization observed at functional
368 level, was not matched by the expression pattern of transporters in sea bass intestine. Thus,
369 revealing that a molecular approach was not enough to profile functional HCO_3^- secretion

characterization on the sea bass intestinal tract. Thus, in the anterior intestine no higher HCO_3^- secretion rates were observed in relation to the mid intestine despite the significant higher expression levels of slc4a4, slc26a6 and slc26a3.This apparent disparity could be accounted for by either post-translational modifications of the proteins, rapid functional activation or membrane recruitment of the transporters in moments of physiological need i.e. feeding (Gregório and Fuentes, 2018).

Regional Na^+/K^+-ATPase and H^+-ATPase activities (Fig. 8) as I_{SC} (Fig. 5) reflected regional active transport potentials and also revealed a functional regional specialization. Basolateral Na^+/K^+-ATPase establishes an electrochemical gradient that promotes Na^+, K^+ and Cl^- uptake by the apical membrane transporters via slc12a1, slc12a3 or Cl^-/HCO_3^- exchangers (reviewed in Grosell and Genz, 2006). In keeping with this idea, the region with higher Na^+/K^+-ATPase activity corresponded to the one with higher slc26a6 and slc26a3 expression levels, as expected. Higher H^+-ATPase activity was observed in the rectum, indicating a higher regional H^+ secretion to the lumen that due to the titration of luminal HCO_3^- likely exported from the mid intestine by peristalsis favours the osmotic gradient for fluid absorption. Regional sea bass I_{SC} represent net Cl^- absorption (Fig. 5) and thus water absorption. Significant decreases in net Cl^- absorption were observed from anterior to posterior regions, being the anterior intestine the region with significant higher Cl^- transepithelial transport. Although Cl^- and water movement occur in the same direction, due to the existence of electroneutral transporters, like slc26a3, slc26a6 and slc12a3, water absorption could be modulated without modifying I_{SC} (Ando et al., 2014). Functionally, the basolateral slc12a2 and the apical slc12a1 could be activated differentially to produce net absorption or secretion (Marshall et al., 2002). On the basolateral side, a Na^+ gradient established by Na^+/K^+-ATPase is the driving force for Cl^- secretion by increasing the intracellular Cl^- concentrations. In sea bass rectum significantly higher slc12a2 expression levels promoted the enhancement of intracellular Cl^- levels, despite the regional lower ATPase activity, explaining the capacity of the tissue to switch to secretory currents.

396 The non-existent or at least non-measurable *in vitro* HCO_3^- secretion in sea bass rectum
397 could be due to several factors. A gene expression profile along the sea bass intestinal tract
398 demonstrated transcriptional regional differences, in which carbonic anhydrase 4 was listed as one
399 of the 30 genes most up-regulated (218.15 fold-change) in the proximal regions in comparison to
400 the posterior segment that included the rectum (Calduch-Giner et al., 2016), indicating that in sea
401 bass rectum the HCO_3^- intracellular contribution was impaired. Furthermore, significantly higher
402 H^+- ATPase activities and expression levels, together with the residual molecular expression of
403 slc4a4, slc26a6 and slc26a3 (Fig. 9) involved in the transcellular pathway, probably were not
404 enough to enable apical HCO_3^- secretion. Although in other species, like SW Senegalese sole, Gulf
405 toadfish, SW rainbow trout and SW Mozambique tilapia, both factors did not compromise HCO_3^-
406 secretion or the luminal HCO_3^- content in the rectum (Grosell et al., 2007; Guffey et al., 2011; Ruiz-
407 Jarabo et al., 2017, 2016). The low HCO_3^- accumulation in the lumen of the rectum (Fig. 3) was
408 probably the result of the H^+ apical efflux in combination with HCO_3^- dehydration by luminal and
409 membrane bound carbonic anhydrases that promoted water absorption (Grosell, 2011; Grosell et al.,
410 2009a, 2009b; Ruiz-Jarabo et al., 2016; Whittamore et al., 2010). In parallel we also observed that
411 intestinal fluid Cl^- concentrations significantly decreased into the distal regions (Fig. 2) after
412 slc12a1 active functioning in the anterior regions. So, to uphold water absorption, Cl^- secretion into
413 the lumen should be promoted in the distal regions to supply slc12a1 and slc12a3, since the Cl^-
414 uptake by these transporters would be compromised (Ando et al., 2014). In sea bass the absence of
415 differences on regional slc12a1 molecular expression and significantly increased expression levels
416 of the two isoforms of slc12a3 in the distal regions, indicated that slc12a3 could be supplementing
417 the transport by slc12a1 in the rectum, securing water absorption, as already suggested for SW
418 Japanese eel and European eel (Ando et al., 2014; Cutler and Cramb, 2008). Taken together these
419 considerations may suggest the existence of a different regional regulatory mechanism present in
420 sea bass rectum yet to be exposed.
421 The existence of different regulatory mechanisms in the sea bass discrete intestinal regions
422 was accessed, we used extracellular HCO_3^- (Fig. 6) and the second messenger cAMP (Fig. 7) as

423 tools. The effects of basolateral HCO_3^- levels on apical secretion were tested in the anterior and mid
424 intestine covering the physiological relevant range for fish plasma (0 - 20 mM). In both intestinal
425 regions increased basolateral HCO_3^- concentrations promoted HCO_3^- secretion, revealing a linear
426 correlation between these two factors ($R^2 > 0.976$, Fig. 6). Increasing the basolateral HCO_3^-
427 concentration to 10 mM, we obtained HCO_3^- secretion values of 600 nmol h^{-1} cm^{-2}, that did not
428 match those reported by Faggio et al. (2011) of circa 900 nmol h^{-1} cm^{-2} using the same intestinal
429 region. A difference in fish body mass between both studies was noted and could be the cause for
430 this disparity. Here we show a negative correlation between fish body mass and HCO_3^- secretion
431 emerged in *in vitro* experiments using sea bass with different body mass (30 – 1100 g). Smaller
432 animals tend to have higher secretion rates than larger fish, showing an allometric relationship with
433 an $R^2 > 0.82$ (Fig. 4D).
434 In preparations devoid of basolateral CO_2 / HCO_3^- that prevented transcellular routes for
435 apical secretion and therefore was generated from intracellular CO_2 hydration revealed first a
436 prevalent HCO_3^- secretion of circa 180 - 220 nmol h^{-1} cm^{-2}. Second, that the intracellular
437 contribution was sufficient to fuel resting HCO_3^- secretion rates, like in SW rainbow trout where
438 HCO_3^- secretion endured while the integrity of the tissue was maintained (Grosell et al., 2009a).
439 And third, the HCO_3^- uptake into the enterocyte mediated by the basolateral slc4a4 was not a
440 limiting step for apical HCO_3^- secretion in this condition. HCO_3^- sources for apical secretion i.e.
441 cellular vs transcellular are believed to vary amongst species and along the intestinal tract (Ando
442 and Subramanyam, 1990; Dixon and Loretz, 1986; Grosell et al., 2009a; Grosell and Genz, 2006;
443 Wilson and Grosell, 2003). Therefore, although the anterior and mid intestine had similar HCO_3^-
444 secretion rates, HCO_3^- transcellular / intracellular contribution differed between these regions (Fig.
445 6). In the anterior intestine the transcellular pathway was prevalent (66 %), probably due to the
446 slc4a4 higher expression levels being the major HCO_3^- source, the blood. In the mid intestine was
447 established that 50 % of the HCO_3^- secreted was provided *via* transcellular pathways and the
448 remained 50 % from cytosolic CO_2 hydration, agreeing with another study in sea bass. Although

449 Faggio et al. (2011) portrayed a much lower intracellular contribution (20 %) to apical secretion
450 probably due to the use of basolateral saline with twice as high HCO_3^- concentration.
451 cAMP increased intracellular levels on HCO_3^- secretion and I_{SC} were investigated with the
452 application of FK and IBMX, promoting tmACs (Fig. 7). In fish enterocytes were described that
453 risen levels of cAMP by tmACs inhibited HCO_3^- secretion. (Carvalho et al., 2012; Tresguerres et
454 al., 2014, 2010). In our experiments, no cAMP inhibitory effect on mid intestine HCO_3^- secretion
455 was observed contrary to the results obtained in all sea bream intestinal regions, although in both
456 studies similar effects on TEP were obtained (Carvalho et al., 2012). In all sea bass intestinal
457 regions, a significant decline on the Cl^- net absorption (Cl^- secretion was enhanced) was observed,
458 as described for sea bream anterior and mid intestine (Carvalho et al., 2012). In SW killifish, it was
459 demonstrated that this response was mediated by cftr (Marshall et al., 2002), and slc26a6 and
460 slc26a3 were not involved. The variation in sea bass regional cftr expression levels, the equal
461 maximal effect on regional I_{SC} promoted by cAMP, and only sea bass rectum was capable of
462 switching to net Cl^- secretion, indicated that there was a basolateral and not an apical limitation in
463 the distal regions, probably by slc12a2. In Gulf toadfish, the effect of guanylin peptides which are
464 upstream cftr regulators that increase intracellular cAMP levels were evaluated. HCO_3^- secretion
465 decreased in the posterior intestine but no effect was observed in the rectum. Intestinal I_{SC} were
466 reverted from net absorptive to secretory, and water secretion was promoted in both posterior
467 intestine and rectum, but not in the anterior region. The authors suggested that these effects were
468 due to cftr and slc12a2 activation and the inhibition of slc12a1 and slc26a6 (Ruhr et al., 2016, 2015,
469 2014). Interestingly, basolateral slc12a2 expression levels were lower in the anterior intestine (Ruhr
470 et al., 2016), confirming the existence of a basolateral limitation for Cl^- secretion in this region.
471 Therefore, sea bass responses to cAMP stimulation could be a culmination of downstream effects of
472 regulatory events occurring in the proximal regions, or region-specific responses (like a basolateral
473 limitation) that differ in an interspecific manner, depending on regional transporters / receptors
474 distribution or endocrine factors involved in the regulatory pathways.
475

In summary, an intestinal anterior-posterior functional regionalization involved in the HCO_3^- secretion in the sea bass was described, which was verified by the significant differences presented by the discrete intestinal regions in: 1) HCO_3^- secretion rates, 2) tissue bioelectrical parameters, 3) HCO_3^- intestinal fluid composition, 4) I_{SC} 5) Na^+/K^+-ATPase and H^+-ATPase activities, and 6) expression levels of basolateral slc4a4, slc12a2, apical slc26a6, slc26a3, slc12a3, cftr and atp6v1b. Regional regulatory mechanisms were revealed: 1) HCO_3^- transcellular / intracellular contribution differed between proximal regions, 2) there is a negative correlation between fish mass and HCO_3^- secretion rates, 3) cAMP stimulation revealed a basolateral limitation for Cl^- secretion in the distal regions, and 4) different regulatory mechanism in sea bass rectum yet to be exposed.

ACKNOWLEDGEMENTS

We appreciate the technical input of Dr. João Eugenio Reis, Cristovão Nunes and Juan Capaz (Ramalhete Marine Station, CCMar, University of Algarve, Portugal) for fish husbandry. This study was supported by the Ministry of Science and Higher Education and European Social Funds through the Portuguese National Science Foundation (FCT) studentship SFRH/BD/113363/2015 to SG and Project PTDC/MAR-BIO/3034/2014 to JF. CCMar is supported through project UID/Multi/04326/2013.

494 **REFERENCES**

495 Ando, M., Mukuda, T., Kozaka, T., 2003. Water metabolism in the eel acclimated to sea water:
496 from mouth to intestine. Comp. Biochem. Physiol. Part B Biochem. Mol. Biol. 136, 621–633.
497 https://doi.org/10.1016/S1096-4959(03)00179-9

498 Ando, M., Subramanyam, M.V. V., 1990. Bicarbonate transport systems in the intestine of the
499 seawater Eel. J. Exp. Biol. 150, 381–394.

500 Ando, M., Wong, M.K.S., Takei, Y., 2014. Mechanisms of guanylin action on water and ion
501 absorption at different regions of seawater eel intestine. Am. J. Physiol. Integr. Comp. Physiol.
502 307, R653–R663. https://doi.org/10.1152/ajpregu.00543.2013

503 Calduch-Giner, J.A., Sitjà-Bobadilla, A., Pérez-Sánchez, J., 2016. Gene expression profiling reveals
504 functional specialization along the intestinal tract of a carnivorous teleostean fish
505 (*Dicentrarchus labrax*). Front. Physiol. 7, 1–17. https://doi.org/10.3389/fphys.2016.00359

506 Carvalho, E.S.M., Gregório, S.F., Canário, A.V.M., Power, D.M., Fuentes, J., 2015. PTHrP
507 regulates water absorption and aquaporin expression in the intestine of the marine sea bream
508 (*Sparus aurata*, L.). Gen. Comp. Endocrinol. 213, 24–31.
509 https://doi.org/10.1016/j.ygcen.2014.12.011

510 Carvalho, E.S.M., Gregório, S.F., Power, D.M., Canário, A.V.M., Fuentes, J., 2012. Water
511 absorption and bicarbonate secretion in the intestine of the sea bream are regulated by
512 transmembrane and soluble adenylyl cyclase stimulation. J. Comp. Physiol. B 182, 1069–
513 1080. https://doi.org/10.1007/s00360-012-0685-4

514 Cutler, C.P., Cramb, G., 2008. Differential expression of absorptive cation-chloride-cotransporters
515 in the intestinal and renal tissues of the European eel (*Anguilla anguilla*). Comp. Biochem.
516 Physiol. Part B Biochem. Mol. Biol. 149, 63–73. https://doi.org/10.1016/j.cbpb.2007.08.007

517 Dixon, J.M., Loretz, C.A., 1986. Luminal alkalinization in the intestine of the goby. J. Comp.
518 Physiol. B 156, 803–811. https://doi.org/10.1007/BF00694254

519 Evans, D.H., 2008. Teleost fish osmoregulation: what have we learned since August Krogh, Homer

520 Smith, and Ancel Keys. Am. J. Physiol. Regul. Integr. Comp. Physiol. 295, R704–R713.
521 https://doi.org/10.1152/ajpregu.90337.2008

522 Evans, D.H., 2005. The multifunctional fish gill: Dominant site of gas exchange, osmoregulation,
523 acid-base regulation, and excretion of nitrogenous waste. Physiol. Rev. 85, 97–177.
524 https://doi.org/10.1152/physrev.00050.2003

525 Faggio, C., Torre, A., Lando, G., Sabatino, G., Trischitta, F., 2011. Carbonate precipitates and
526 bicarbonate secretion in the intestine of sea bass, *Dicentrarchus labrax*. J. Comp. Physiol. B
527 Biochem. Syst. Environ. Physiol. 181, 517–525. https://doi.org/10.1007/s00360-010-0538-y

528 Ferlazzo, A., Carvalho, E., Gregório, S., Power, D., Canário, A., Trischitta, F., Fuentes, J., 2012.
529 Prolactin regulates luminal bicarbonate secretion in the intestine of the sea bream (*Sparus*
530 *aurata* L.). J. Exp. Biol. 215, 3836–3844. https://doi.org/10.1242/jeb.074906

531 Fuentes, J., Eddy, F.B., 1997. Drinking in marine, euryhaline and freshwater teleost fish, in: Hazon,
532 N., Eddy, F.B., Flik, G. (Eds.), Ionic regulation in animals: A tribute to Professor
533 W.T.W.Potts. Springer Berlin Heidelberg, Berlin, Heidelberg, pp. 135–149.
534 https://doi.org/10.1007/978-3-642-60415-7_9

535 Fuentes, J., Power, D.M., Canário, A. V., 2010. Parathyroid hormone-related protein-stanniocalcin
536 antagonism in regulation of bicarbonate secretion and calcium precipitation in a marine fish
537 intestine. Am. J. Physiol. Regul. Integr. Comp. Physiol. 299, R150-8.
538 https://doi.org/10.1152/ajpregu.00378.2009

539 Giffard-Mena, I., Charmantier, G., Grousset, E., Aujoulat, F., Castille, R., 2006. Digestive tract
540 ontogeny of *Dicentrarchus labrax*: Implication in osmoregulation. Dev. Growth Differ. 48,
541 139–151. https://doi.org/10.1111/j.1440-169X.2006.00852.x

542 Gregório, S., Fuentes, J., 2018. Regulation of bicarbonate secretion in marine fish intestine by the
543 calcium-sensing receptor. Int. J. Mol. Sci. 19, 1072. https://doi.org/10.3390/ijms19041072

544 Gregório, S.F., Carvalho, E.S.M., Campinho, M.A., Power, D.M., Canário, A.V.M., Fuentes, J.,
545 2014. Endocrine regulation of carbonate precipitate formation in marine fish intestine by

546 stanniocalcin and PTHrP. J. Exp. Biol. 217, 1555–1562. https://doi.org/10.1242/jeb.098517

547 Gregório, S.F., Carvalho, E.S.M., Encarnação, S., Wilson, J.M., Power, D.M., Canário, A.V.M.,
548 Fuentes, J., 2013. Adaptation to different salinities exposes functional specialization in the
549 intestine of the sea bream (*Sparus aurata* L.). J. Exp. Biol. 216, 470–479.
550 https://doi.org/10.1242/jeb.073742

551 Grosell, M., 2011. Intestinal anion exchange in marine teleosts is involved in osmoregulation and
552 contributes to the oceanic inorganic carbon cycle. Acta Physiol. 202, 421–434.
553 https://doi.org/10.1111/j.1748-1716.2010.02241.x

554 Grosell, M., 2006. Intestinal anion exchange in marine fish osmoregulation. J. Exp. Biol. 209,
555 2813–2827. https://doi.org/10.1242/jeb.02345

556 Grosell, M., Genz, J., 2006. Ouabain-sensitive bicarbonate secretion and acid absorption by the
557 marine teleost fish intestine play a role in osmoregulation. Am. J. Physiol. Integr. Comp.
558 Physiol. 291, R1145–R1156. https://doi.org/10.1152/ajpregu.00818.2005

559 Grosell, M., Genz, J., Taylor, J.R., Perry, S.F., Gilmour, K.M., 2009a. The involvement of H^+-
560 ATPase and carbonic anhydrase in intestinal HCO_3^- secretion in seawater-acclimated rainbow
561 trout. J. Exp. Biol. 212, 1940–1948. https://doi.org/10.1242/jeb.026856

562 Grosell, M., Gilmour, K.M., Perry, S.F., 2007. Intestinal carbonic anhydrase, bicarbonate, and
563 proton carriers play a role in the acclimation of rainbow trout to seawater. Am. J. Physiol.
564 Regul. Integr. Comp. Physiol. 293, R2099–R2111. https://doi.org/10.1152/ajpregu.00156.2007

565 Grosell, M., Laliberte, C.N., Wood, S., Jensen, F.B., Wood, C.M., 2001. Intestinal HCO_3^- secretion
566 in marine teleost fish: Evidence for an apical rather than a basolateral Cl^-/HCO_3^- exchanger.
567 Fish Physiol. Biochem. 24, 81–95. https://doi.org/10.1023/A:1011994129743

568 Grosell, M., Mager, E.M., Williams, C., Taylor, J.R., 2009b. High rates of HCO_3^- secretion and Cl^-
569 absorption against adverse gradients in the marine teleost intestine: the involvement of an
570 electrogenic anion exchanger and H^+-pump metabolon? J. Exp. Biol. 212, 1684–1696.
571 https://doi.org/10.1242/jeb.027730

572 Grosell, M., Taylor, J.R., 2007. Intestinal anion exchange in teleost water balance. Comp. Biochem.
573 Physiol. Part A Mol. Integr. Physiol. 148, 14–22. https://doi.org/10.1016/j.cbpa.2006.10.017

574 Guffey, S., Esbaugh, A., Grosell, M., 2011. Regulation of apical H^+-ATPase activity and intestinal
575 HCO_3- secretion in marine fish osmoregulation. Am. J. Physiol. Regul. Integr. Comp. Physiol.
576 301, R1682–R1691. https://doi.org/10.1152/ajpregu.00059.2011

577 Jensen, M.K., Madsen, S.S., Kristiansen, K., 1998. Osmoregulation and salinity effects on the
578 expression and activity of Na^+,K^+-ATPase in the gills of European sea bass, *Dicentrarchus*
579 *labrax* (L.). J. Exp. Zool. 282, 290–300. https://doi.org/10.1002/(SICI)1097-
580 010X(19981015)282:3<290::AID-JEZ2>3.0.CO;2-H

581 Kurita, Y., Nakada, T., Kato, A., Doi, H., Mistry, A.C., Chang, M.-H., Romero, M.F., Hirose, S.,
582 2008. Identification of intestinal bicarbonate transporters involved in formation of carbonate
583 precipitates to stimulate water absorption in marine teleost fish. Am. J. Physiol. Regul. Integr.
584 Comp. Physiol. 294, R1402-12. https://doi.org/10.1152/ajpregu.00759.2007

585 Larkin, M.A., Blackshields, G., Brown, N.P., Chenna, R., Mcgettigan, P.A., McWilliam, H.,
586 Valentin, F., Wallace, I.M., Wilm, A., Lopez, R., Thompson, J.D., Gibson, T.J., Higgins, D.G.,
587 2007. Clustal W and Clustal X version 2.0. Bioinformatics 23, 2947–2948.
588 https://doi.org/10.1093/bioinformatics/btm404

589 Loretz, C.A., 1995. Electrophysiology of ion transport in teleost intestinal cells, in: Fish physiology.
590 Academic Press, pp. 25–56. https://doi.org/10.1016/S1546-5098(08)60241-1

591 Louro, B., Marques, J.P., Power, D.M., Canário, A.V.M., 2016. Having a BLAST: Searchable
592 transcriptome resources for the gilthead sea bream and the European sea bass. Mar. Genomics
593 30, 67–71. https://doi.org/10.1016/j.margen.2016.10.004

594 Marshall, W.S., Grosell, M., 2006. Ion transport, osmoregulation, and acid–base balance, in: The
595 physiology of fishes. pp. 179–214.

596 Marshall, W.S., Howard, J.A., Cozzi, R.R., Lynch, E.M., 2002. NaCl and fluid secretion by the
597 intestine of the teleost *Fundulus heteroclitus*: involvement of CFTR. J. Exp. Biol. 205, 745–

758.

Martos-Sitcha, J.A., Campinho, M.A., Mancera, J.M., Martinez-Rodriguez, G., Fuentes, J., 2015. Vasotocin and isotocin regulate aquaporin 1 function in the sea bream. J. Exp. Biol. 218, 684–693. https://doi.org/10.1242/jeb.114546

McCormick, S.D., 1993. Methods for nonlethal gill biopsy and measurement of Na^+, K^+ -ATPase activity. Can. J. Fish. Aquat. Sci. 50, 656–658. https://doi.org/10.1139/f93-075

McCormick, S.D., Farrell, A.P., Brauner, C.J., 2013. Fish Physiology: Euryhaline fishes, Vol 32. Academic Press. ISBN**:** 9780123972323

Musch, M.W., Orellana, S.A., Kimberg, L.S., Field, M., Halm, D.R., Krasny, E.J., Frizzell, R.A., 1982. Na^+-K^+-Cl^- co-transport in the intestine of a marine teleost. Nature 300, 351–353. https://doi.org/10.1038/300351a0

Parmelee, J.T., Renfro, J.L., 1983. Esophageal desalination of seawater in flounder: role of active sodium transport. Am. J. Physiol. Integr. Comp. Physiol. 245, R888–R893. https://doi.org/10.1152/ajpregu.1983.245.6.R888

Ruhr, I.M., Bodinier, C., Mager, E.M., Esbaugh, A.J., Williams, C., Takei, Y., Grosell, M., 2014. Guanylin peptides regulate electrolyte and fluid transport in the Gulf toadfish (*Opsanus beta*) posterior intestine. Am. J. Physiol. Integr. Comp. Physiol. 307, R1167–R1179. https://doi.org/10.1152/ajpregu.00188.2014

Ruhr, I.M., Mager, E.M., Takei, Y., Grosell, M., 2015. The differential role of renoguanylin in osmoregulation and apical Cl^- /HCO_3^- exchange activity in the posterior intestine of the Gulf toadfish (*Opsanus beta*). Am. J. Physiol. Regul. Integr. Comp. Physiol. 309, 399–409. https://doi.org/10.1152/ajpregu.00118.2015

Ruhr, I.M., Takei, Y., Grosell, M., 2016. The role of the rectum in osmoregulation and the potential effect of renoguanylin on SLC26a6 transport activity in the Gulf toadfish (*Opsanus beta*). Am. J. Physiol. Integr. Comp. Physiol. 311, R179–R191. https://doi.org/10.1152/ajpregu.00033.2016

624 Ruiz-Jarabo, I., Barany-Ruiz, A., Jerez-Cepa, I., Mancera, J.M., Fuentes, J., 2016. Intestinal
625 response to salinity challenge in the Senegalese sole (*Solea senegalensis*). Comp. Biochem.
626 Physiol. Part A Mol. Integr. Physiol. 204, 57–64. https://doi.org/10.1016/j.cbpa.2016.11.009

627 Ruiz-Jarabo, I., Gregório, S.F., Gaetano, P., Trischitta, F., Fuentes, J., 2017. High rates of intestinal
628 bicarbonate secretion in seawater tilapia (*Oreochromis mossambicus*). Comp. Biochem.
629 Physiol. -Part A Mol. Integr. Physiol. 207, 57–64. https://doi.org/10.1016/j.cbpa.2017.02.022

630 Smith, H.W., 1931. The absorption and excretion of water and salts by the elasmobranch fishes.
631 Am. J. Physiol. - Leg. Content 98, 279–295.

632 Taylor, J.R., Grosell, M., 2006. Evolutionary aspects of intestinal bicarbonate secretion in fish.
633 Comp. Biochem. Physiol. Part A Mol. Integr. Physiol. 143, 523–529.
634 https://doi.org/10.1016/j.cbpa.2006.01.027

635 Taylor, J.R., Mager, E.M., Grosell, M., 2010. Basolateral NBCe1 plays a rate-limiting role in
636 transepithelial intestinal HCO_3^- secretion, contributing to marine fish osmoregulation. J. Exp.
637 Biol. 213, 459–468. https://doi.org/10.1242/jeb.029363

638 Tresguerres, M., Barott, K.L., Barron, M.E., Roa, J.N., 2014. Established and potential
639 physiological roles of bicarbonate-sensing soluble adenylyl cyclase (sAC) in aquatic animals.
640 J. Exp. Biol. 217, 663–672. https://doi.org/10.1242/jeb.086157

641 Tresguerres, M., Levin, L.R., Buck, J., Grosell, M., 2010. Modulation of NaCl absorption by
642 [HCO_3^-] in the marine teleost intestine is mediated by soluble adenylyl cyclase. Am. J. Physiol.
643 Integr. Comp. Physiol. 299, R62–R71. https://doi.org/10.1152/ajpregu.00761.2009

644 Walsh, P.J., Blackwelder, P., Gill, K.A., Danulat, E., Mommsen, T.P., 1991. Carbonate deposits in
645 marine fish intestines: A new source of biomineralization. Limnol. Oceanogr. 36, 1227–1232.
646 https://doi.org/10.4319/lo.1991.36.6.1227

647 Whittamore, J.M., 2012. Osmoregulation and epithelial water transport: Lessons from the intestine
648 of marine teleost fish. J. Comp. Physiol. B Biochem. Syst. Environ. Physiol. 182, 1–39.
649 https://doi.org/10.1007/s00360-011-0601-3

Whittamore, J.M., Cooper, C.A., Wilson, R.W., 2010. HCO_3^- secretion and $CaCO_3$ precipitation play major roles in intestinal water absorption in marine teleost fish *in vivo*. Am. J. Physiol. Integr. Comp. Physiol. 298, R877–R886. https://doi.org/10.1152/ajpregu.00545.2009

Wilson, R.W., Grosell, M., 2003. Intestinal bicarbonate secretion in marine teleost fish - source of bicarbonate, pH sensitivity, and consequences for whole animal acid-base and calcium homeostasis. Biochim. Biophys. Acta - Biomembr. 1618, 163–174. https://doi.org/10.1016/j.bbamem.2003.09.014

Wilson, R.W., Wilson, J.M., Grosell, M., 2002. Intestinal bicarbonate secretion by marine teleost fish - why and how? Biochim. Biophys. Acta - Biomembr. 1566, 182–193. https://doi.org/10.1016/S0005-2736(02)00600-4

661 **Table 1** – Ion composition (mM) and osmolality (mOsm Kg^{-1}) of sea bass plasma and intestinal
662 fluid. All values represent mean ± SEM for n = 10 individuals (337.4 ± 15.6 g body mass). *
663 indicate significant differences between plasma and intestinal fluid ($p < 0.01$, unpaired t-test).

	Plasma concentration (mM)	**Intestinal fluid concentration (mM)**
Sodium	176 ± 1.4	62.9 ± 6.8 *
Chloride	147 ± 3.0	91.9 ± 5.9 *
Potassium	3.8 ± 0.20	6.7 ± 0.85
Phosphorus	2.7 ± 0.07	2.3 ± 0.60
Calcium	1.51 ± 0.03	12.8 ± 0.48 *
Magnesium	1.09 ± 0.06	141 ± 8.5 *
Osmolality (mOsm Kg^{-1})	336 ± 4.9	337 ± 8.5

664

665 **Table 2** – Composition of basolateral and apical salines used in the Ussing chambers experiments.

	HCO_3^- free Basolateral saline (mM)	**Basolateral saline (mM)**	**Apical saline (mM)**
NaCl	147	147	61
Na-Gluconate	19	19	-
Na_2HPO_4	-	-	1
KH_2PO_4	3	3	-
KCl	-	-	5
$MgSO_4$	1.1	1.1	142
$CaCl_2$	1.5	1.5	13
Glucose	5	5	-
HEPES	5	5	-
$NaHCO_3$	-	5	-
Na-HEPES	10	5	-
Osmolality (mOsmol l^{-1})	340*	340*	340*

666 * adjusted with mannitol to ensure transepithelial isosmotic conditions

667

668 **Table 2** – Primers (Fw-forward; Rv-Reverse) used for qPCR expression analysis, length of PCR
669 products (bp) and corresponding NCBI accession numbers or the Sea Blast Server identifiers
670 provided by the transcriptome database (http://sea.ccmar.ualg.pt in Louro et al., 2016).

Gene		Primer Sequence (5' to 3')	Size (bp)	Accession No.
18S	FW	AACCAGACAAATCGCTCCAC	139	**AY993930**
	RV	CCTGCGGCTTAATTTGACTC		
atp6v1b	FW	TACAGCGCTGAGAACTTTGC	124	**AY532636.1**
	RV	GGTTCAAGAAAAGGCAGACG		
slc4a4	FW	AACGATAGTCCCACCACCAC	118	lcl|SRR_TRINITY_DN78630_c0_g1_i3
	RV	CGTCTCTCGGCAACTTCTTC		
slc26a6	FW	GTGGACAGCAACCAGGAACT	119	lcl|SRR15_isotig08512
	RV	CCTCCTGTGCTCTCCTGAAC		
slc26a3	FW	CTGTGGAGAAGGGACAAACC	120	lcl|ERR_TRINITY_DN115547_c3_g1_i3
	RV	GACGACACTGATCAGCTCCA		
Cftr	FW	GATGATCCTGGGAGAGTTGGT	131	**DQ501276**
	RV	CATAGGTCAGGCCAAACAAGA		
slc12a2	FW	GGCTGTAGCCATGTATGTGGT	131	**AY954108**
	RV	CCAGGAGCAGGATTACTGTGA		
slc12a1	FW	CATTTTACGCAGCTGTGGTCT	131	lcl|ERR_TRINITY_DN114503_c1_g2_i1
	RV	GCTCGAAGTCCTCCAGTCTCT		
slc12a3-001	FW	CAAACGGAAGCTGAAGTCGT	138	lcl|SRR_TRINITY_DN81540_c0_g1_i3
	RV	CGCCAGTCTCTCTTGAAACC		
slc12a3-002	FW	GGGAGTCCAAGACCCAGATT	125	**JN635474**
	RV	ACTGCGGTATCCAAAGATG		

671

672

673 **FIGURE LEGENDS**

674 **Figure 1.** Photograph depicturing carbonate precipitates in the intestine of the sea bass. Discrete
675 intestinal regions schematic: the anterior intestine, which extends from the pyloric caeca 3 – 6 cm;
676 the mid intestine, represents 53 - 58 % of the intestine total length, that is recognizable by its
677 thinner musculature, and terminates at the ileo-rectal sphincter; and the rectum, which is delimited
678 by the ileo-rectal and anal sphincters, with 2 – 3.5 cm of length. The measurements indicated
679 correspond to individuals with body weights ranging between 250 - 1300 g.

680 **Figure 2.** Ion composition (mM) of the luminal fluid of sea bass discrete intestinal regions. All
681 values represent mean ± SEM for n = 10 - 12 individuals (499.2 ± 71.5 g body mass). * indicate
682 significant differences with the anterior region and ** between all discrete intestinal regions ($p <$
683 0.01, two-way ANOVA followed by the Bonferroni post-hoc test).

684 **Figure 3.** Characterization of HCO_3^- content in intestinal fluid (mEq l^{-1}, 3A) and in $Ca(Mg)CO_3$
685 precipitates (nEq body $mass^{-1}$, 3B) in the sea bass intestinal lumen. Results are shown as mean ±
686 SEM for n = 11 individuals (829.7 ± 96.90 g body mass). Bars displaying different superscript
687 letters are significantly different ($p < 0.05$, one-way ANOVA followed by the Bonferroni post-hoc
688 test).

689 **Figure 4.** Basal HCO_3^- secretion (nmol h^{-1} cm^{-2}, 4A) for at least 30 min stable period in the sea bass
690 discrete intestinal regions, and corresponding bioelectrical parameters: transepithelial potential
691 (TEP, mV, 4B) and conductance (G_t, mS cm^{-2}, 4C), considering the voltage referenced to the apical
692 side of the preparation. Results are shown as mean ± SEM for n = 11 - 13 individuals (218.6 ± 65.6
693 g body mass). Bars displaying different superscript letters are significantly different ($p < 0.05$), one-
694 way ANOVA followed by the Bonferroni post-hoc test). Mid intestine HCO_3^- secretion (nmol h^{-1}
695 cm^{-2}) and corresponding fish body mass class (g) logarithmic regression (4D) for 34 individuals in
696 which is displayed the regression equation and R-squared value.

Figure 5. Basal short circuit current (I_{SC}, μA cm^2, 5A) for at least 30 min stable period in the sea bass discrete intestinal regions, and corresponding transepithelial conductance (G_t, mS cm^{-2}, 5B) as measured in Ussing chambers under voltage clamp. Results are shown as mean ± SEM for n = 21 individuals (364.2 ± 43.6 g body mass). Bars displaying different superscript letters are significantly different ($p < 0.01$, one-way ANOVA followed by the Bonferroni post-hoc test).

Figure 6. HCO_3^- secretion (nmol h^{-1} cm^{-2}, 6A) in the sea bass anterior and mid intestine of at least 30 min stable period in basal control conditions (basolateral saline with 5 mM HCO_3^-), in response to the basolateral addition (till 10 and 20 mM final concentration) or withdraw of HCO_3^- (saline substitution of HCO_3^- with HEPES, bubbled with 100 % O_2). In which is also displayed the linear regressions of each intestinal region (black dashed line) between the HCO_3^- secretion rates and different basolateral HCO_3^- concentrations (regression equations: Anterior intestinal HCO_3^- secretion = 64.68 * basolateral [HCO_3^-] + 190.7 with $R^2 = 0.9758$; Mid intestinal HCO_3^- secretion = 46.8 * basolateral [HCO_3^-] + 197.1 with $R^2 = 0.9864$), as well as the percentage of different HCO_3^- sources contribution in basal conditions. Corresponding bioelectrical parameters: transepithelial potential (TEP, mV, 6B) and conductance (G_t, mS cm^{-2}, 6C). Results are shown as mean ± SEM, the number of individuals is indicated adjacent to the x axis. Bars displaying different superscript letters represent significant differences for each intestinal region ($p < 0.05$, one-way ANOVA followed by the Bonferroni post-hoc test).

Figure 7. Effect of 10 μM FK + 500 μM IBMX addition to sea bass intestine (represented by time = 0): Short circuit current (I_{SC}, μA cm^2, 7A) in response to bilateral addition of 10 μM FK + 500 μM IBMX to sea bass discrete intestinal regions, and corresponding maximal effect on I_{SC} (7B) and transepithelial conductance (G_t, mS cm^{-2}, 7C). HCO_3^- secretion (nmol h^{-1} cm^{-2}, 7D) in response to basolateral addition of 10 μM FK + 500 μM IBMX to the sea bass mid intestine, and corresponding bioelectrical parameters: transepithelial potential (TEP, mV, 7E) and conductance (G_t, mS cm^{-2}, 7F). Results are shown as mean ± SEM for n = 10 - 13 (7A - C) and 6 - 7 (7D - F) individuals. ** represent statistical differences from the treatment (7A, D-F) or between intestinal regions (7B - C)

723 ($p < 0.01$, one-way ANOVA (7A - C) and two-way ANOVA (7D -F) both followed by the
724 Bonferroni post-hoc test).

725 **Figure 8**. Na^+/K^+- ATPase (µmolADP mg $protein^{-1}$ h^{-1}, 8A) and H^+-ATPase (µmolADP mg $protein^{-1}$ h^{-1}, 8B) activities in discrete regions of the sea bass intestine. Results are shown as mean ± SEM
727 for n = 8 individuals. Bars displaying different superscript letters represent significant differences ($p < 0.05$, one-way ANOVA RM followed by the Bonferroni post-hoc test).

729 **Figure 9**. Relative expression (gene of interest / reference gene 18S) of atp6v1b (9A), slc4a4 (9B),
730 slc26a6 (9C), slc26a3 (9D), slc12a2 (9E), slc12a1 (9F), slc12a3-001 (9G), slc12a3-002 (9H) and
731 cftr (9I) in discrete intestinal regions of juvenile sea bass. Results are shown as mean ± SEM for n =
732 8 individuals. Bars displaying different superscript letters represent significant differences ($p <$
733 0.05, one-way ANOVA followed by the Bonferroni post-hoc test).

734

Figure 1. Alves et al.

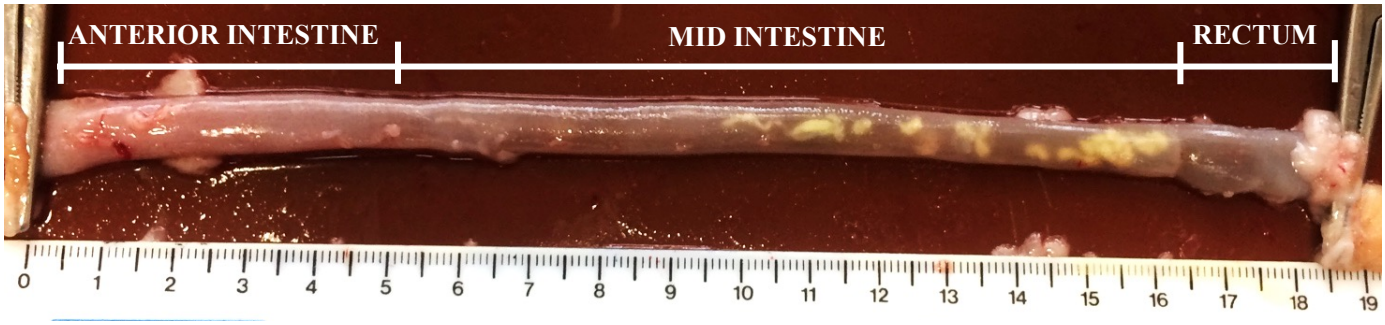

740 **Figure 2.** Alves et al.

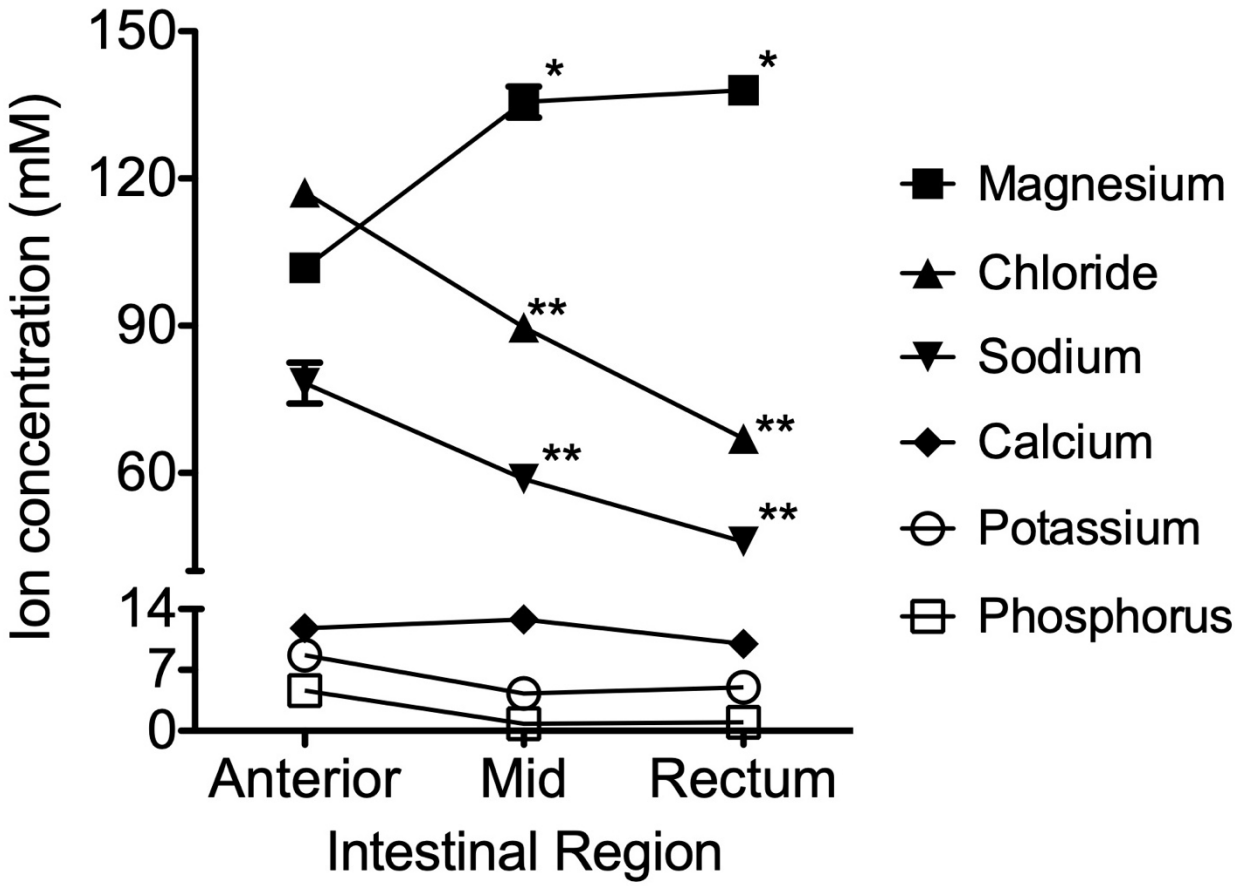

741

742

743 **Figure 3.** Alves et al.

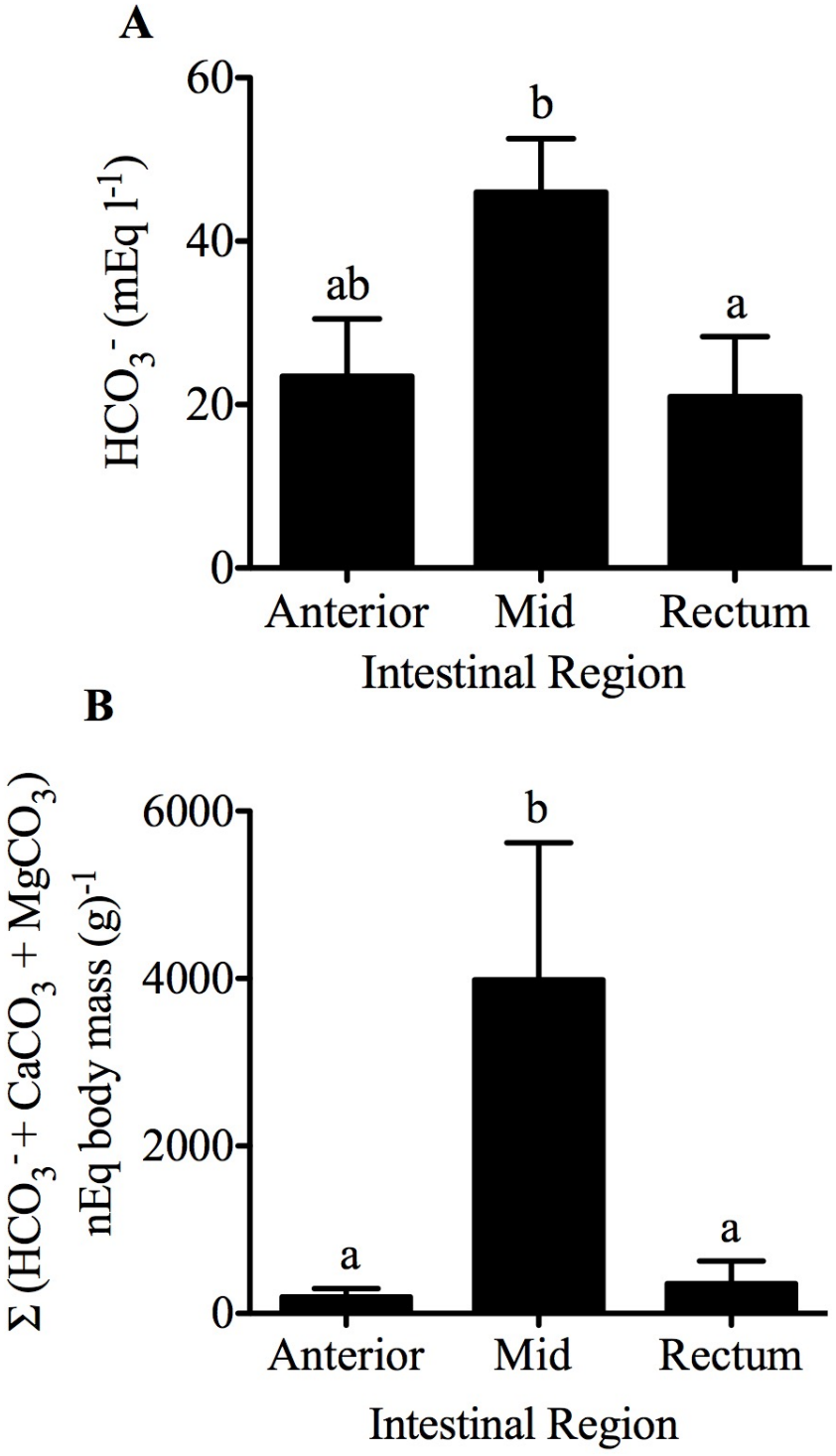

744

745

746 **Figure 4.** Alves et al.

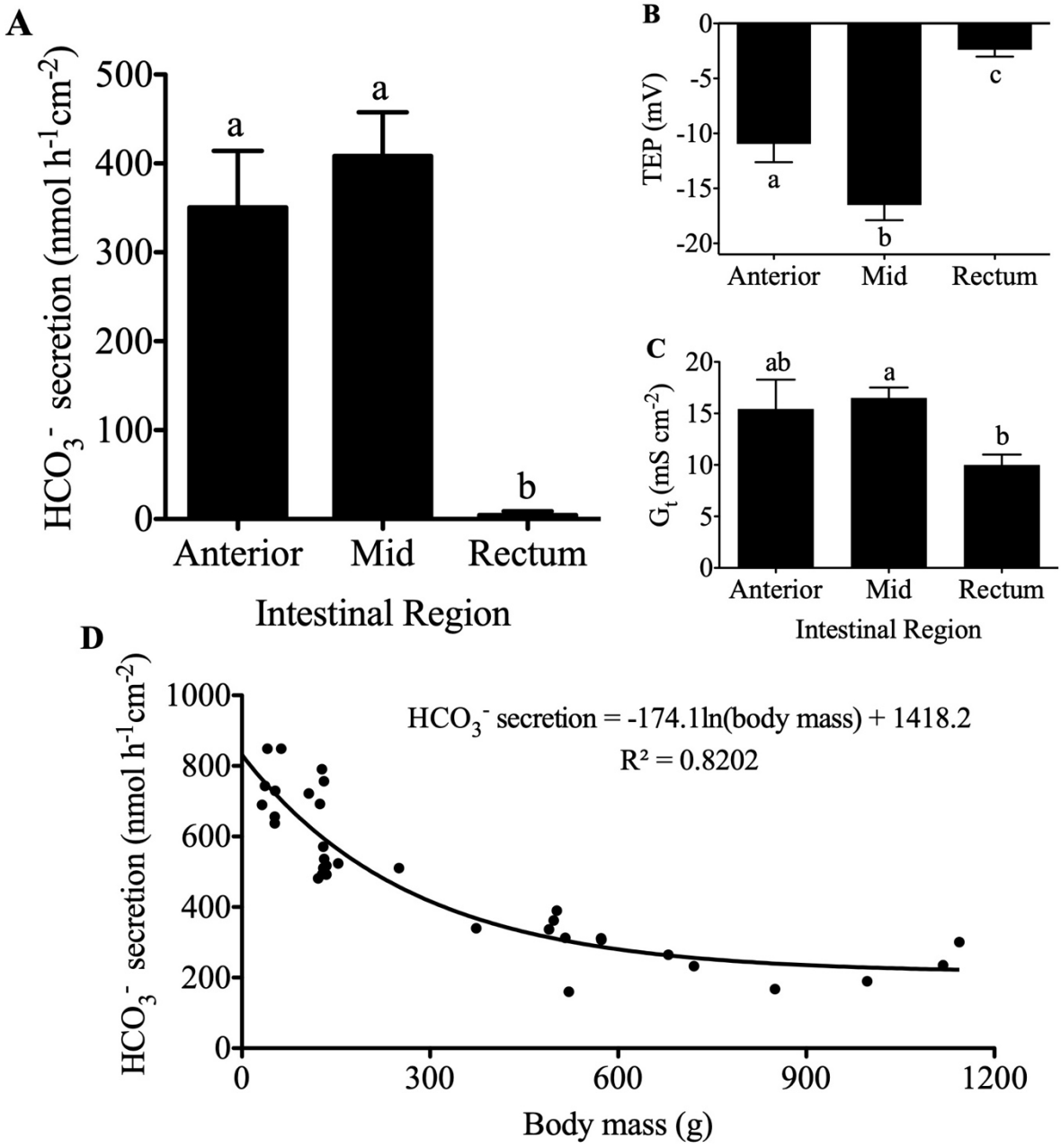

747

748

749 **Figure 5.** Alves et al.

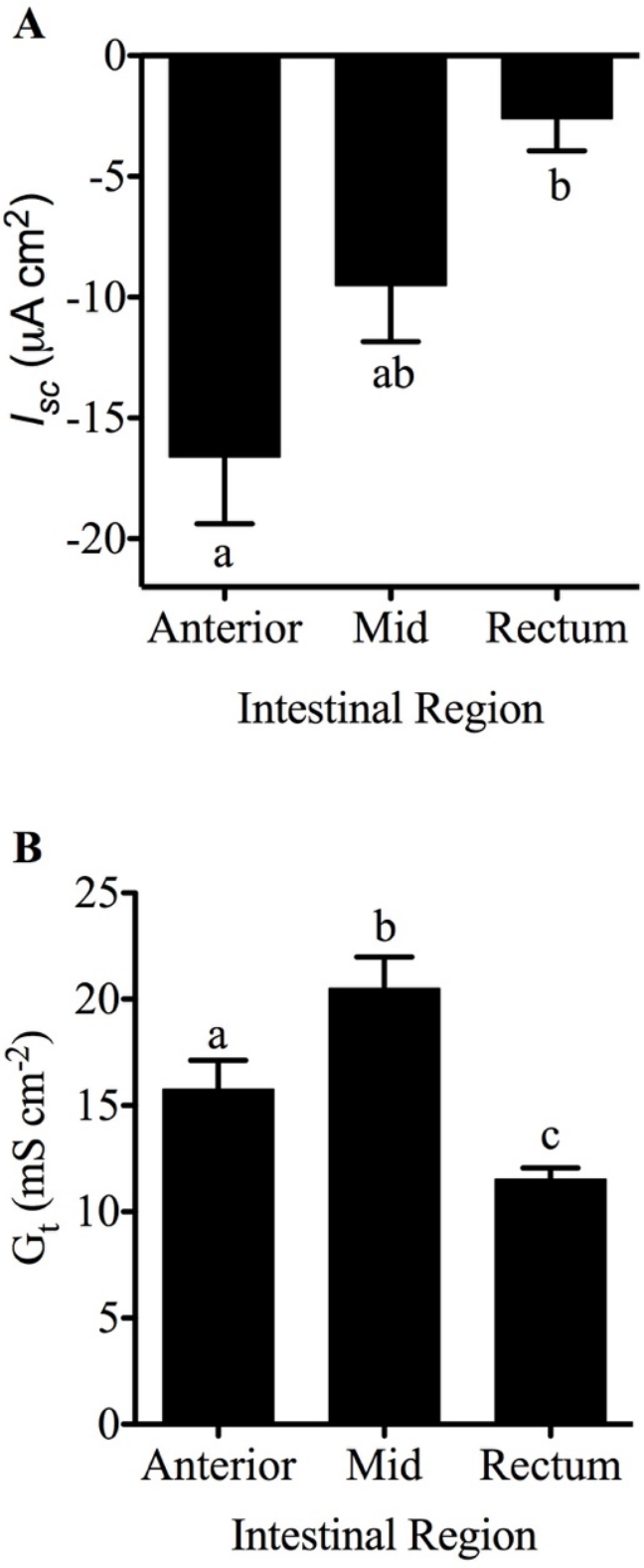

750

751

752 **Figure 6.** Alves et al.

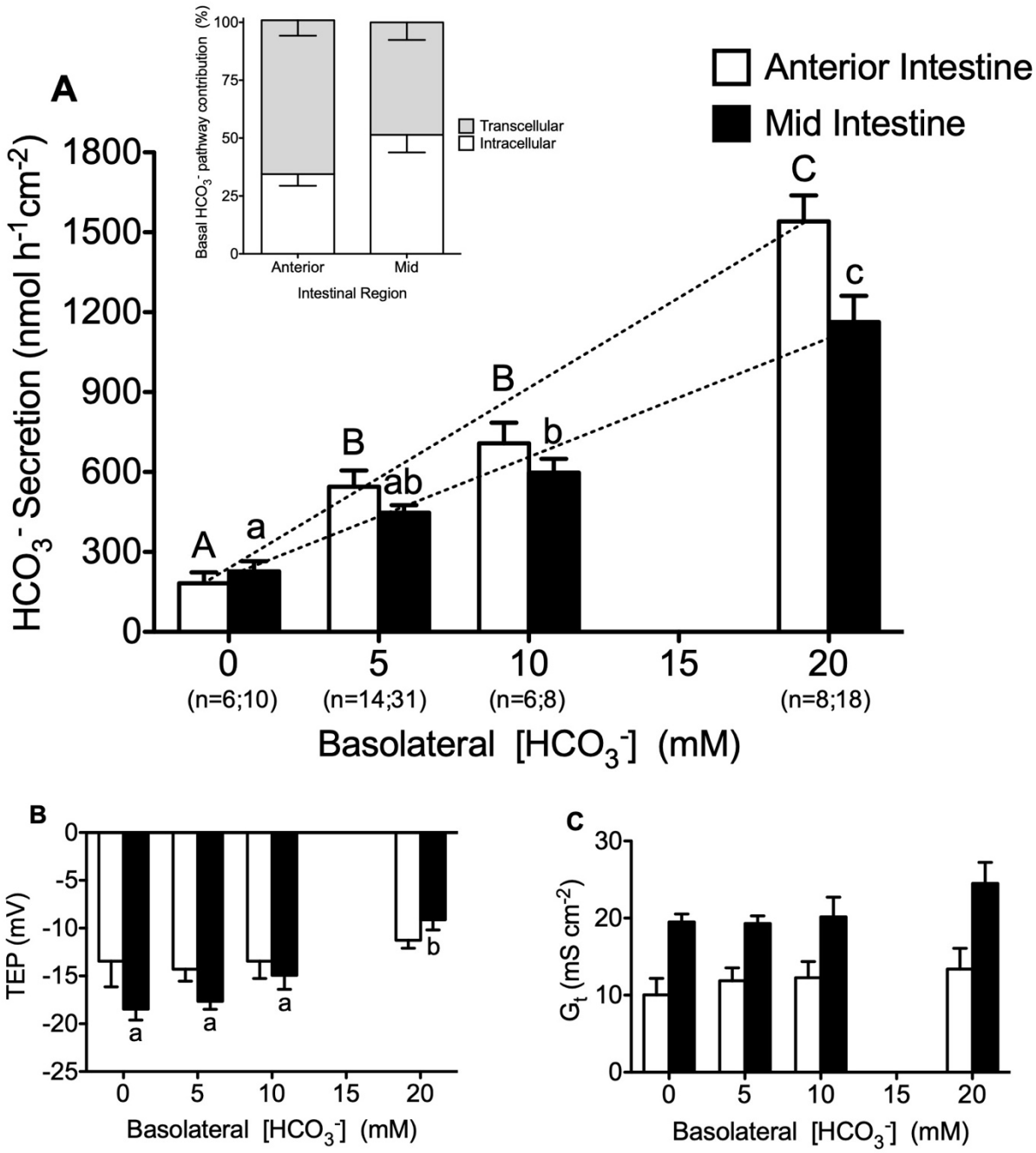

753

754

755 **Figure 7.** Alves et al.

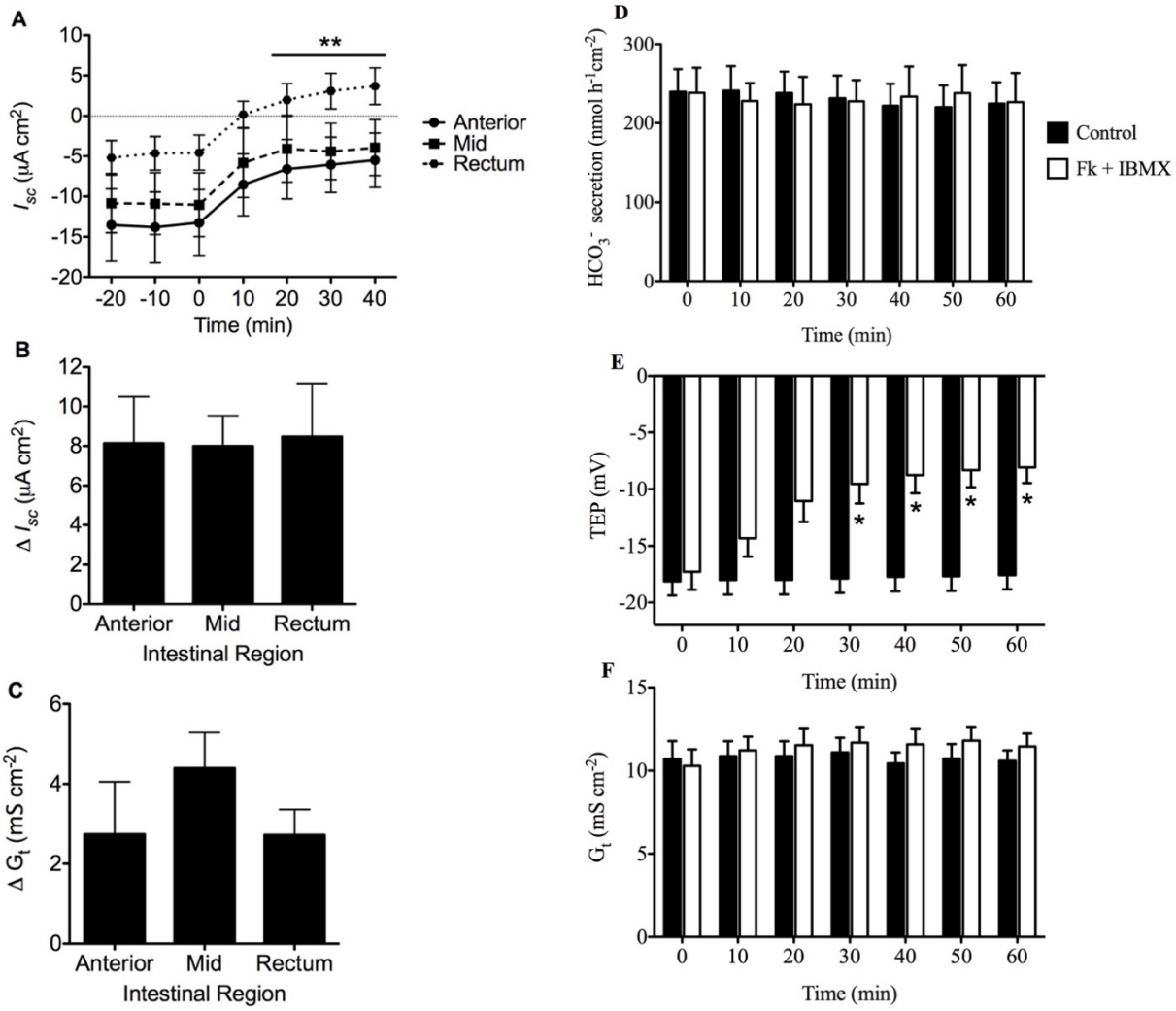

756

757

758

759 **Figure 8.** Alves et al.

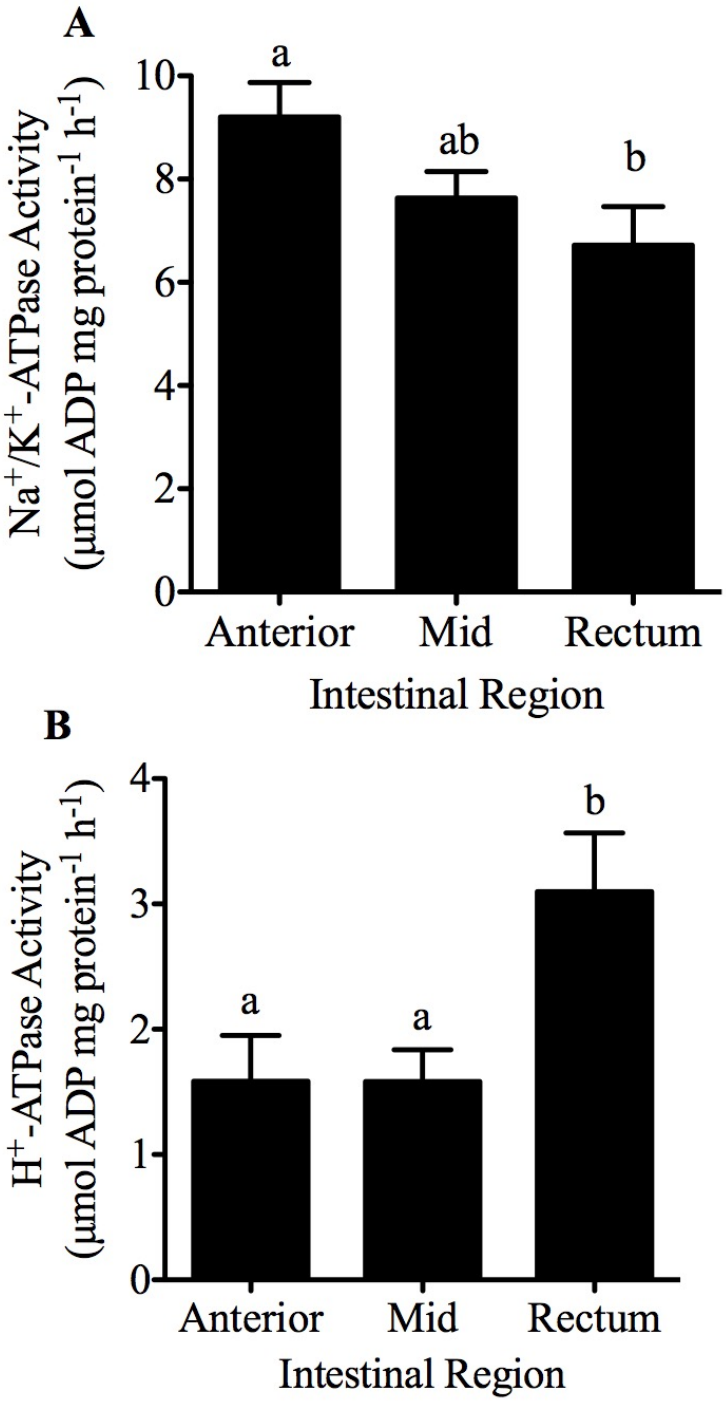

760

761

762 **Figure 9.** Alves et al.

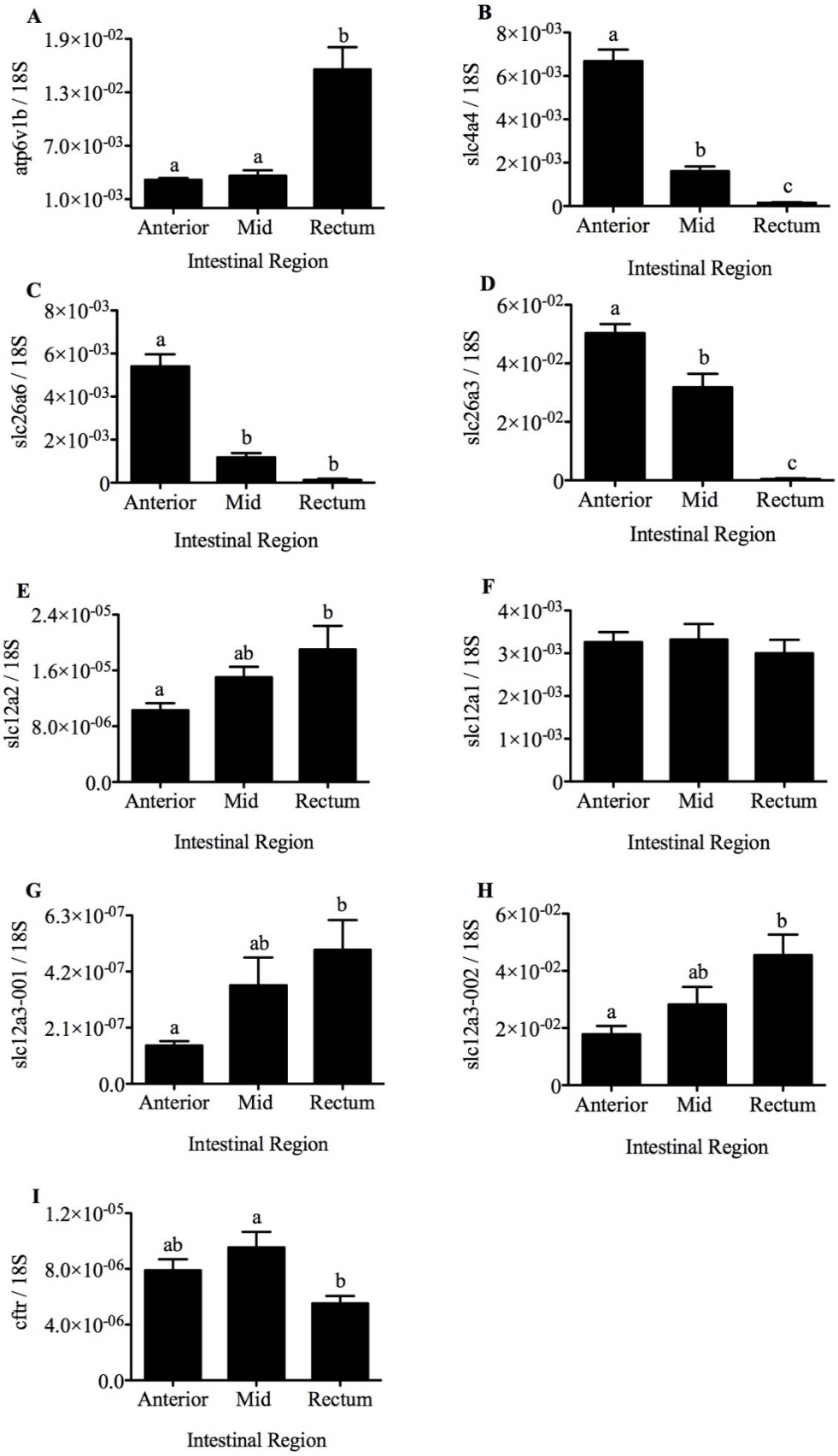

763